Journal of Applied Polymer Science

Nanosized Cellulose Derivatives as Green Reinforcing Agents at Higher Loadings in Natural Rubber

Sonal Thakore
Department of Chemistry, Faculty of Science, Maharaja Sayajirao University of Baroda, Vadodara 390 002, India
Correspondence to: S. Thakore (E-mail: chemistry2797@yahoo.com)

ABSTRACT: Cellulose nanoparticles (CelNPs) prepared by an acid hydrolysis process were acetylated under ambient conditions to retain the nanosize and to obtain hydrophobic nanosized derivatives. Green nanocomposites of natural rubber (NR) with more than 50 phr of cellulosic fillers were successfully developed by a commercial dry mixing process. The incorporation of cellulose acetate nanofiller up to 40 phr led to an almost linear increase in both the tensile and elongation properties, which were higher than even those of a composite with the conventional filler carbon black (CB). This was further supported by the almost uniform single-phase morphology of the nanobiocomposite revealed by scanning electron microscopy and the high thermal stability. The results indicate the high degree of compatibility between the hydrophobic nanosized filler and the NR matrix. Although a drop in the mechanical strength was observed above 50 phr, the cellulose derivatives were expected to prove to be promising substitutes for the hazardous filler CB even at higher loadings. © 2014 Wiley Periodicals, Inc. J. Appl. Polym. Sci. **2014**, *131*, 40632.

KEYWORDS: mechanical properties; nanoparticles; nanowires and nanocrystals; thermal properties

Received 26 September 2013; accepted 20 February 2014
DOI: 10.1002/app.40632

INTRODUCTION

Natural rubber (NR), as a renewable natural resource, has many excellent comprehensive properties, including an outstanding resilience, high strength, and good processability. NR is reinforced with fillers, notably carbon black (CB), silica, or calcium-based powders, to achieve enhanced mechanical performance. Generally, an increase in the modulus is achieved at the expense of the strength and the elongation at break. There are some exceptions, particularly CB, which is an excellent reinforcing agent because of its strong interaction with rubbers.[1] CB is manufactured by burning oil or natural gas in controlled conditions. Because of more environmentally aware consumers, the increased price of crude, and global warming, CB is increasingly being substituted by cheaper and more environmentally friendly inorganic particles, such as silica.[2] However, inorganic fillers have a much reduced affinity toward the elastomer components and, thus, tend to form large aggregates; this leads to drawbacks in processing and poor reinforcement. Hence, inorganic sources of biomass are increasingly being looked upon as another potential source of CB.[3,4]

The reinforcement of polymer materials with polysaccharides is being extensively studied because of their renewable character, low density, and availability and the diversity of their sources.[5] Among polysaccharides, cellulose (Cel) is the most abundant renewable organic material produced in the biosphere. It has been reported that colloidal suspensions of Cel can be obtained by controlled sulfuric acid catalyzed degradation of Cel fibers.[6] The disordered or paracrystalline regions of Cel are preferentially hydrolyzed, whereas its crystalline regions remain intact.[7] Cellulose nanoparticles (CelNPs) obtained by acid hydrolysis have been used as fillers in various polymers, including important elastomers such as NR.[8] However, the main hurdle for using Cel as a reinforcing phase is its hydrophilicity. Because of an abundance of hydroxyl groups at the surface of the Cel, chemical modifications, such as esterification, etherification, oxidation, silylation, and polymer grafting, have been attempted.[9–11] The amphiphilic nature thus imparted upon Cel gives it a wide and interesting application spectrum. However, many of these modifications require vigorous or prolonged reaction conditions, which may also lead to the agglomeration of nanocrystals.[12]

Rubber-based nanocomposites have been studied to a limited extent compared to plastic-based ones, with most of the research focusing on the use of either nanoclays or carbon nanotubes as reinforcements.[13,14] To obtain a uniform dispersion in the rubbery matrix, different processing methods, such as solution casting, latex blending, two-roll mill mixing, and

Additional Supporting Information may be found in the online version of this article.

melt mixing, have been attempted.[15,16] However, very few NR-based nanocomposites with biobased nanoreinforcements, such as chitin whiskers, starch nanocrystals, Cel whiskers extracted from *Syngonanthus nitens* (Capim Dourado), rachis of the palm tree, sisal, and bagasse, are found in literature.[17,18] Extensive work on the bionanocomposites of NR has been reported by Dufresne et al.[19,20] However, most of these studies have used a latex blending technique without vulcanization, and the content of the polysaccharide is generally low. There have been hardly any reports on vulcanized rubber-based Cel nanocomposites prepared by master-batch processing and two-roll mill mixing; these have the potential to be adapted for commercial use.

Our group has focused on highlighting the reinforcing ability of various polysaccharides, including starch, by employing commercial mixing methods.[21–23] Starch derivatives have been found to induce excellent reinforcement in NR up to filler loadings of 30 phr. In this study, the development of nanocomposites highly filled (>50 phr) with cellulosic fillers was attempted. To improve their compatibility with NR and to preserve the nanosize, the room-temperature acetylation of the CelNPs was carried out for the first time by the authors. The resulting hydrophobic derivative was used for the development of highly filled bionanocomposites with NR by dry mixing. The reinforcing performance of the modified Cel derivatives was compared with that of native Cel and commercial-grade CB.

EXPERIMENTAL

Materials

Cel, cellulose acetate (CelAc), sulfuric acid, acetic anhydride, *p*-toluene sulfonic acid, and acetic acid were purchased from Sigma Aldrich (Bombay). NR and high-abrasion furnace-grade CB (N330) with a particle size of 28–36 nm were kindly supplied by Mouldtech Rubber Industries (Vadodara).

Experimental Procedure

For the synthesis of the CelNPs, a known weight of Cel was mixed with 3.16*M* H_2SO_4, and the suspension was stirred continuously for 5 days. The nanoparticles were collected by centrifugation and washed repeatedly with distilled water until they were neutral. They were stored under refrigeration at 4°C with 0.5 mL of chloroform. These nanoparticles (CelNPs) were used to synthesized cellulose acetate nanoparticles (CelAcNPs).

To a mixture of CelNPs and acetic acid, acetic anhydride was added dropwise at room temperature. After a few minutes of stirring, *p*-toluene sulfonic acid was added, and the reaction mass was maintained with stirring for 1 h at 60°C. The product was centrifuged, washed with distilled water, and dried at 50°C *in vacuo*.

Four sets of biocomposites were prepared with each of Cel, CelNPs, CelAc, and CelAcNPs as reinforcing fillers in NR by dry process on two-roll mixing.[23] For the sake of comparison, composites with commercial-grade CB were also prepared. Up to 60 phr of fillers were added along with other additives, namely, sulfur (1.8 phr), tetramethylene thiuram disulfide (0.5 phr), mercaptobenzothiazyl disulfide (1 phr), zinc oxide (5 phr), and stearic acid (1 phr). Mastication was continued until homogeneous composites were obtained. This was followed by vulcanization at 150°C and at about 300 kPa of pressure for 7–8 min to obtain composite sheets that were 1 mm thick.

Characterization

The shape and size of the nanoparticles were determined by a Philips Technai 20 model transmission electron microscope (Holland) operating at 200 kV. We prepared the sample for transmission electron microscopy (TEM) by putting one drop of the colloidal solution onto standard carbon-coated copper grids and then drying under an electric bulb for 30 min. X-ray diffraction (XRD) was determined with a PANalytical X'Pert-PRO XRPD. Fourier transform infrared (FTIR) spectra of the vacuum-dried nanoparticles were recorded as the KBr pellet on the PerkinElmer RX1 model.

The curing properties were measured in a Monsanto R-100 rheometer at a temperature of 150°C according to ISO 3417. The shore hardness was measured on a Frank hardness tester with a shore A durometer at several points on the surface of the specimen. An average of six measurements was taken as the result. The stress–strain properties of all of the NR composites were measured on a universal testing machine (Lloyd Instruments) with a test specimen in the form of dumbbells according to ASTM standard and procedure D 412. The gauge length was 50.0 mm. The crosshead speed was 10 mm/min at 25°C and 50% humidity. The data given are the average of five measurements. The fraction of bound rubber was determined by the following procedure.[24] A specimen 1 mm thick and 1 cm in diameter was cut from the master batches and put into a previously weighed cage made of 280-mesh stainless-steel wire gauze. The cage was soaked in the solvent for 72 h. The cage was taken out after 72 h and air-dried. The bound rubber content (R_B) was calculated with the following equation:

$$R_B = W_{tg} - W\left[m_f/\left(m_f + m_p\right)\right]/W\left[m_p/\left(m_f + m_p\right)\right] \times 100$$

where W_{tg} is the weight of the filler and gel, W is the weight of the specimen, m_f is the weight of the filler in the compound, and m_p is the weight of the polymer.

The surface morphology of the tensile fractured surfaces was examined by means of a JEOL scanning electron microscope (JEOL JSM-5610LV) with a conductive coating of carbon. An accelerating potential of 15 kV was used for the analysis of the sample. Thermogravimetric analysis (TGA) was recorded on a TG–DTA 6300 INCARP EXSTAR 6000 in a nitrogen atmosphere in the temperature range from 30 to 450°C at a heating rate of 10°C/min. Differential scanning calorimetry (DSC) was performed on DSC 60 Shimadzu in a nitrogen atmosphere in the temperature range of −80 to 0°C at a heating rate of 10°C/min. For each sample, two different specimens were characterized, and it was shown that the DSC thermograms superimposed perfectly. Dynamic mechanical analysis (DMA) was carried out with a Netzsch DMA 242. The specimen was a thin rectangular strip (15 × 5.1 × 0.959 mm^3). The analysis was carried out in the temperature range of −90° to 25°C at a frequency of 1 Hz in a nitrogen atmosphere. The setup measured the complex tensile modulus, that is, the storage modulus (E') and the loss modulus (E''). The ratio between the two components, the loss factor (tan δ), was also determined. Sorption studies were

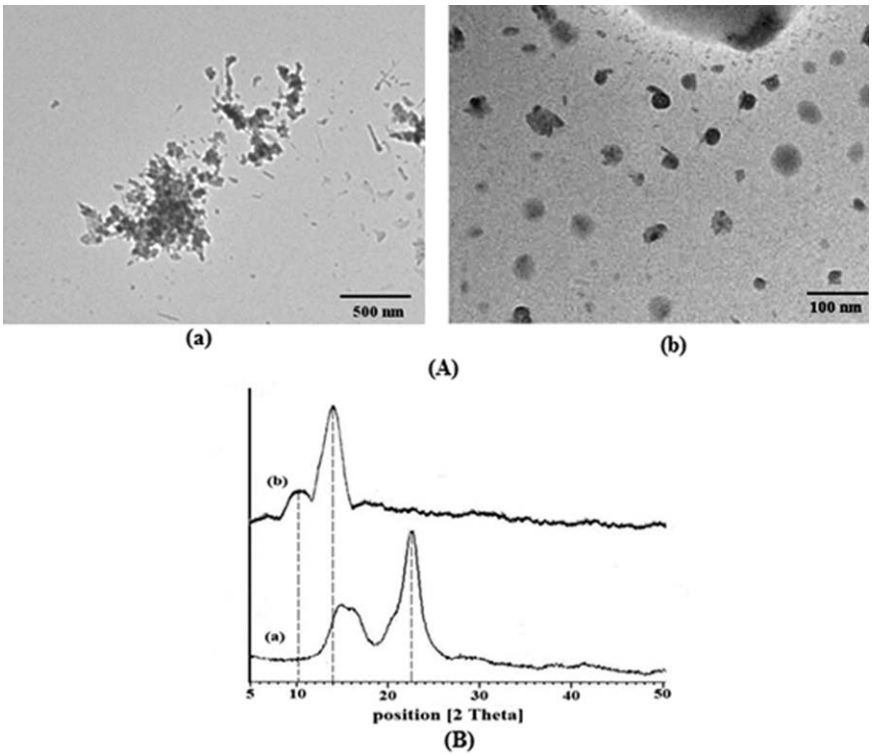

Figure 1. (A) TEM image and (B) XRD spectra of the (a) CelNPs and (b) CelAcNPs.

performed in water and the nonpolar solvent toluene to determine the degree of hydrophobicity by a method reported elsewhere.[23]

RESULTS AND DISCUSSION

TEM images of the nanocrystals before and after modification are shown in Figure 1(A). Thicker bundles of fibrils around 70–80 nm corresponding to bigger Cel aggregates were observed along with some individual fibrils [Figure 1(A-a)]. After the modification process, the crystallinity of the CelNPs was lost, and 25–30-nm spherical particles were observed [Figure 1(A-b)]. The particles were more individualized and monodisperse compared to their unmodified counterparts. The CelNPs were also believed to aggregate as a result of hydrogen-bond interactions due to the surface hydroxyl groups. These interactions were blocked after modification, which decreased the polar contribution and improved the individualization of nanoparticles.[25] Hence, the CelAcNPs were smaller in size compared to the unmodified counterparts.

Figure 1(B) shows the XRD pattern of the Cel and CelAcNPs. The peaks at 14.89 and 22.6° were characteristic of Cel[26] [Figure 1(B-a)]. Although in the case of acetylated CelNPs, peaks at 10.4 and 13.2° were observed [Figure 1(B-b)]. This suggested that the crystallinity of the CelNPs was destroyed after the modification, and the hydroxyl groups were replaced by acetyl groups.

In the FTIR spectra of the CelNPs [Figure 2(A)], the peak at 3400 cm^{-1} was due to —OH stretching, and the peak at 1640 cm^{-1} was due to tightly bound water.[23] Although the absorption band between 1000 and 1200 cm^{-1} were characteristic of the —C—O stretching of the polysaccharide skeleton. In acetylated CelNPs, a strong absorption peak at 1736 cm^{-1} was attributed to the stretching of ester carbonyl >C═O [Figure 2(B)]. The intensity of the peak corresponding to 3400 cm^{-1} decreased; this indicated that the acetylation process took place. The other peak around 1200 cm^{-1} was attributed to the —C—O—C— bond stretching of the ether linkage.[27]

Whenever there was excessive mastication, the viscosity registered a sharp decrease. Normally, the maximum torque in the rheograph can be taken as the maximum viscosity of the rubber compounds, and it is a relative measure of the crosslinking density in the samples.[28] The processability of the composites could be studied from the rheographs. Here, the representative rheograph showed that the curing time of the composites was around 6–7 min (Figure S1, Supporting Information).

The Shore hardness measurements showed that in all of the composites, the hardness increased with increased filler loading. The results show that up to 30 phr, all four fillers showed superior hardness to CB. After this, the hardness increased but was less than that of CB/NR. CelAcNPs/NR imparted the best hardness properties followed by CelAc/NR, CelNPs/NR, and Cel/NR (Table I).

The mechanical properties of the composites were evaluated in terms of the tensile strength and percentage elongation, as shown in Figure 3(A,B). The values for the ultimate tensile strength and percentage elongation for unfilled rubber were 0.58 MPa and 41%, respectively. At 10 phr, the cellulosic fillers imparted a very high tensile strength and very high elongation

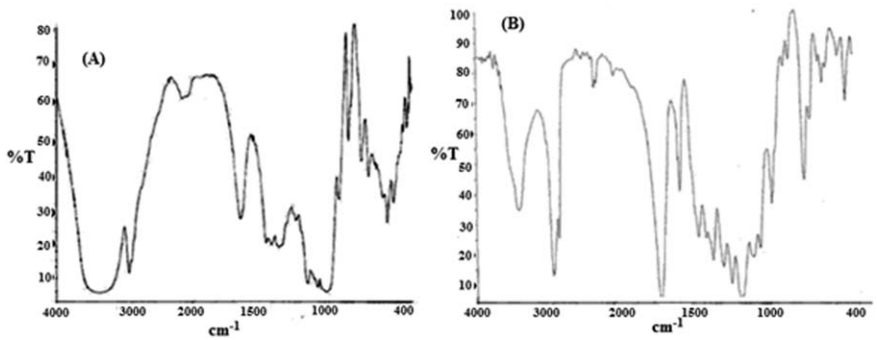

Figure 2. FTIR spectra of the (A) CelNPs and (B) CelAcNPs.

properties compared to CB. As the filler loading increased, there was a steep rise in the mechanical properties of the CB composites. This increase was gradual in the case of the Cel composites, except for those containing CelAcNPs. Among all of the fillers, the CelAcNPs exhibited the best reinforcing ability up to 50 phr and preserved the elastic behavior of the nanocomposites. At still higher loadings, the performance of CB was observed to be very superior to the cellulosic fillers. The results of the mechanical properties testing also indicate that the combined effect of the size reduction and organic modification drastically improved the filler–matrix adhesion and, hence, the performance of Cel.

The results of the mechanical properties could be explained on the basis of morphology. The SE micrographs of the fractured samples of the composites at 40-phr loading are shown in Figure 4. The scanning electron microscopy image of the Cel/NR composite showed the presence of the particles on the surface, which may have leached out during fracture [Figure 4(A)]. The CelAc/NR composite revealed somewhat homogeneous surface characteristics; this indicated filler–matrix compatibility [Figure 4(B)]. The CB/NR composite showed a two-phase morphology and the presence of holes formed during fracture, as evident from Figure 4(C). Against this, the nanofillers were more evenly distributed in the polymer matrix [Figure 4(D,E)]. In case of the unmodified CelNPs/NR nanocomposite, the reduction in size compensated for the hydrophilic nature [Figure 4(D)]. Among them, the CelAcNPs/NR nanocomposite appeared to show an almost single-phase morphology; this did not reveal any particles on the surface [Figure 4(E)]. This probably indicated that the filler particles were deeply embedded in the matrix. The decrease in the mechanical properties of the CelAcNPs/NR nanocomposite at 60 phr may have been due to the formation of aggregates of excessive filler, which resulted in an improper distribution. This was evident from the micrograph in Figure 4(F), which shows the occurrence of holes similar to those seen in the CB/NR composite at 40 phr.

The results of bound rubber (Table S1) were in accordance with the mechanical properties. The bound rubber was found out to be highest in case of the composite containing CelAcNPs as the filler, although at 60 phr, the bound rubber was found to be greater in the composite containing CB as a filler compared instead of the CelAcNPs.

The thermal stability is a crucial factor when polysaccharides are used as reinforcing agents because they suffer from inferior thermal properties compared to inorganic fillers. Because vulcanization is carried out at high temperatures, it is important that the alteration of the surface chemistry does not decrease the thermal stability. The TGA curves shown in Figure 5 clearly show that the acetylation increased the thermal stability of Cel because of the decreased number of hydroxyl groups.[29]

The TGA data of all of the composites at 60-phr loading showed an initial mass loss from 150 to 250°C. This was attributed to the elimination of volatile components such as water.[30] The degradation temperatures of the biocomposites were in close proximity with those of the CB composites. This may have been because high vulcanization temperatures may have resulted in some extent of crosslinking within the polysaccharide network. The results also show that the modified Cel imparted better thermal stability to the composites compared to native Cel. As already observed in the mechanical properties because of the combined effect of the size reduction and organic modification, the decomposition temperatures of the CelAcNPs/NR nanocomposite were even higher than those of the CB/NR

Table I. Hardness Data for the Composites

	Shore A Hardness					
Composite	10	20	30	40	50	60
Cel/NR	40	44	45	48	49	51
CelAc/NR	43	44	46	49	52	55
CelNPs/NR	41	45	47	49	51	53
CelAcNPs/NR	43	46	49	53	55	58
CB/NR	28	38	47	54	59	63

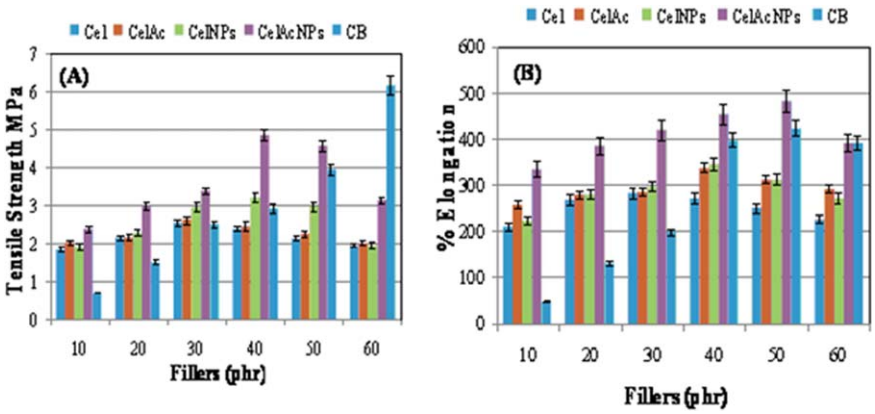

Figure 3. (A) Tensile strength and (B) elongation of composites containing various fillers. [Color figure can be viewed in the online issue, which is available at wileyonlinelibrary.com.]

composite (Table II). This was due to the increase in the onset temperature as compared to other composites (data not shown); this led to an increase in the thermal stability.

DSC analysis of the NR composites at a 60-phr filler loading showed that the biocomposites had a glass-transition temperature (T_g) comparable with that of the CB/NR composite (Table II), whereas that of the unfilled NR was around $-66°C$.[30] T_g also continued to increase with the filler loading as expected (data not shown). The T_g of the CelAcNPs/NR nanocomposite was highest because of its hydrophobic nature and small size, which imparted rigidity and strength to the network.

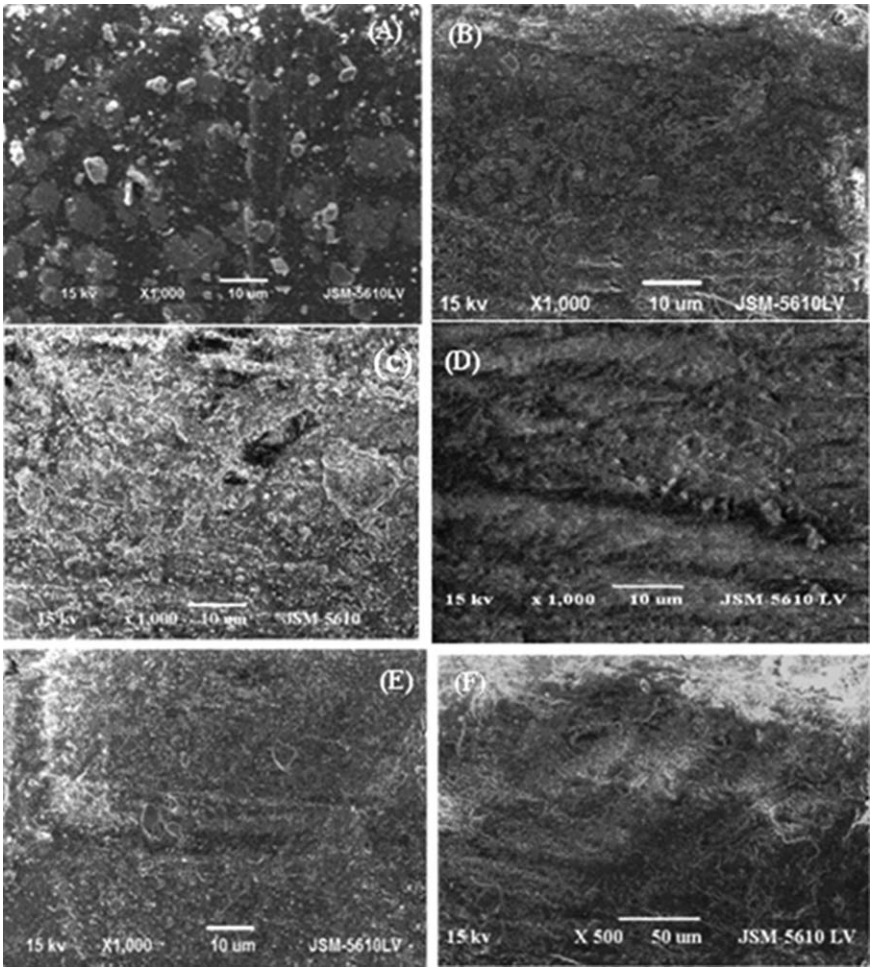

Figure 4. Scanning electron micrographs of the NR composites with 40-phr loadings of the (A) Cel, (B) CelAc, (C) CB, (D) CelAcNPs, and (E) CelNPs and with a 60-phr loading of the (F) CelAcNPs.

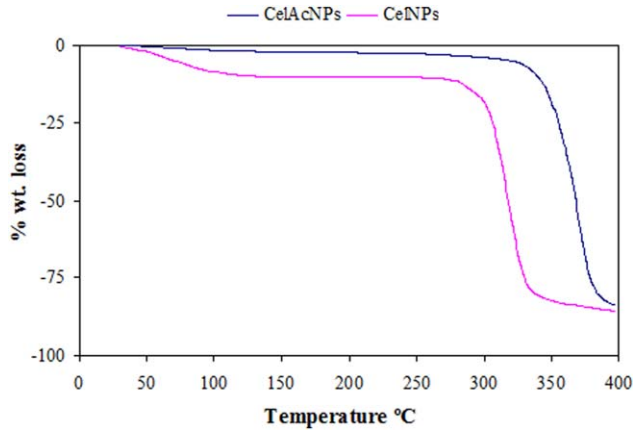

Figure 5. TGA curves of the nanoparticles. [Color figure can be viewed in the online issue, which is available at wileyonlinelibrary.com.]

Figure 6 shows the DMA spectra [tan δ, Figure 6(A)] and logarithm of dynamic E' [log E'; Figure 6(B)] values of the CelAcNPs/NR nanocomposite at a 60-phr loading as a function of the temperature at 1 Hz. A sharp decrease was observed around −62°C; this corresponded to the primary relaxation process associated with the glass–rubber transition determined by DSC measurements. In this temperature range, the loss angle passed through a maximum [Figure 6(A)]. At low temperature, that is, below T_g, the reinforcing effect of the cellulosic nanoparticles was low; this justified the normalization of the modulus. Above T_g, a much more significant reinforcing effect of nanoparticles was observed. DMA involved weak stresses, and the adhesion between the filler and the matrix was not damaged.

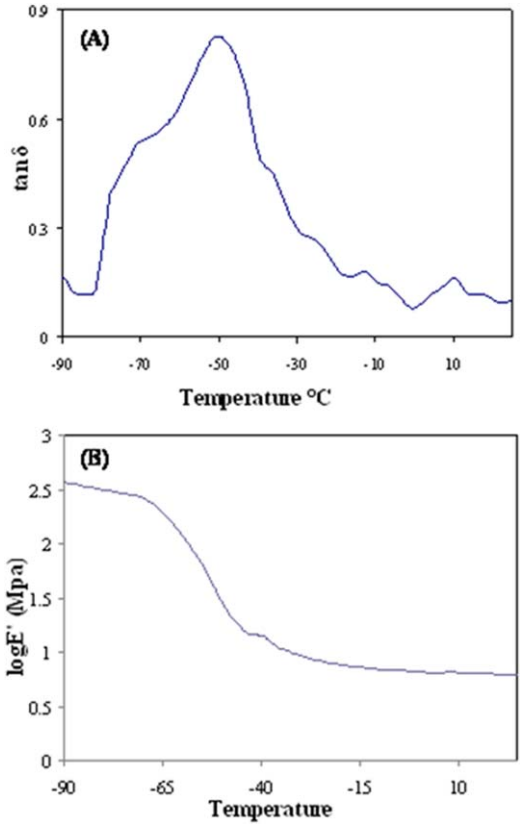

Figure 6. Effect of the nanocomposite containing 60-phr CelAcNPs on (A) the mechanical tan δ and (B) the logarithm of E' versus the temperature. [Color figure can be viewed in the online issue, which is available at wileyonlinelibrary.com.]

Table II. Thermogravimetry Data and T_g Values for the NR Composites Containing Various Fillers

	Degradation temperature at weight loss (°C)					
Filler	1%	2%	5%	10%	50%	T_g at 60 phr (°C)
Cel	137	191	257	288	325	−62.96
CelNPs	161	202	271	309	359	−62.06
CelAc	145	198	266	297	357	−62.81
CelAcNPs	187	222	286	312	369	−61.88
CB	114	192	264	304	364	−62.24

Table III. Water and Toluene Sorption of the NR Composites Containing Various Fillers

	Molar uptake (%)					
	Water			Toluene		
Filler	20 phr	40 phr	60 phr	20 phr	40 phr	60 phr
Cel	2.81	1.94	1.07	2.77	2.19	1.76
CelNPs	1.05	0.56	0.25	2.56	2.11	1.67
CelAc	1.37	0.88	0.31	2.86	2.33	1.87
CelAcNPs	0.87	0.31	0.17	2.85	2.22	1.81
CB	0.71	0.42	0.22	2.38	1.61	1.12

Under higher stress, as used for the tensile tests, the adhesion was involved. The tan δ curve of the CelAcNPs/NR nanocomposite showed a broad relaxation process from −90 to 25°C. This may have been due to the relaxation of the rubber fraction confined inside the layers.[8]

The filler–matrix adhesion and the components embedded in the matrix were important factors in the determination of the sorption behavior of the composite. In cellulosic composites, the water sorption was expected to increase with the amount of filler. However, the results demonstrated in Table III show that the water uptake decreased with the amount of filler. The adsorption of macromolecular chains at the filler–matrix interface through interactions between the CelNPs and NR could reduce swelling. Indeed, the formation of a three-dimensional network was already reported for polysaccharide nanoparticles.[8] It may have resulted from hydrogen-bonding forces between the unreacted hydroxyl groups of nanoparticles during the vulcanization. At higher loadings, nanoparticles connected to form an infinite percolating network; this could have been a barrier limiting the diffusion of toluene within the material. A fraction of the matrix material thus became inaccessible for swelling (entrapped NR fraction). Similar results were obtained for starch-filled nanocomposites in the past.[23] This indicated that the interaction between the polymer matrix and filler led to the formation of a bound polymer in close proximity to the reinforcing filler; this restricted the solvent uptake. However, this hypothesis needs deeper analysis.

CONCLUSIONS

The study led to the conclusion that filler–matrix adhesion dominated the performance of the fillers. CelAcNPs with the special advantage of nanosize and hydrophobicity exhibited the best mechanical strength, with the optimum being at 40 phr. Similar to CB composites, the water sorption of the biocomposites was found to decrease linearly, independent of the nature of the filler. Furthermore, the polysaccharides did not lead to significant thermal degradation of the composite, whereas acetylation improved the thermal stability. We concluded that the CelAcNPs could be potential green reinforcing agents, even at higher loadings.

ACKNOWLEDGMENTS

The authors are grateful to the Council of Scientific and Industrial Research (New Delhi, India) for its financial assistance.

REFERENCES

1. Angellier, H.; Molina-Boisseau, S.; Lebrun, L.; Dufresne, A. *Macromolecules* **2005**, *38*, 9161.
2. Wang, Z. F.; Peng, Z.; Li, S. D.; Lin, H.; Zhang, K. X.; She, X. D.; Fu, X. *Compos. Sci. Technol.* **2009**, *69*, 1797.
3. Filson, P. B.; Dawson-Andoh, B. E. *Bioresour. Technol.* **2009**, *100*, 2259.
4. Corrales, F.; Vilaseca, F.; Llop, M.; Girones, J.; Mendez, J. A.; Mutje, P. *J. Hazard. Mater.* **2007**, *144*, 730.
5. Dufresne, A. *J. Nanosci. Nanotechnol.* **2006**, *6*, 322.
6. Habibi, Y.; Lucia, A. L.; Rojas, O. J. *Chem. Rev.* **2010**, *110*, 3479.
7. Angles, M. N.; Dufresne, A. *Macromolecules* **2001**, *34*, 2921.
8. Bendahou, A.; Kaddami, H.; Dufresne, A. *Eur. Polym. J.* **2010**, *46*, 609.
9. Fan, X.; Liu, Z. T.; Liu, Z. W. *J. Hazard. Mater.* **2010**, *177*, 452.
10. Lee, K. Y.; Quero, F.; Blacker, J. J.; Hill, C. A. S.; Eichhorn, S. J.; Bismarck, A. *Cellulose* **2011**, *18*, 595.
11. Berlioz, S.; Molina-Boisseau, S.; Nishiyama, Y.; Heux, L. *Biomacromolecules* **2009**, *10*, 2144.
12. Xu, Y.; Ding, W.; Liu, J.; Li, Y.; Kennedy, J. F.; Gu, Q.; Shao, S. *Carbohydr. Polym.* **2010**, *80*, 1078.
13. Anand, A. K.; Jose, S. T.; Alex, R.; Joseph, R. *Int. J. Polym. Mater.* **2010**, *59*, 33.
14. Wang, Y.; Zhang, H.; Wu, Y.; Yang, J.; Zhang, L. *J. Appl. Polym. Sci.* **2005**, *96*, 318.
15. Hajji, P.; Cavaille, J. Y.; Favier, V.; Gauthier, C.; Vigier, G. *Polym. Compos.* **1996**, *17*, 4.
16. Bras, J.; Hassan, M. L.; Cecile, B.; Hassan, E. A.; El-Wakil, N. A.; Dufresne, A. *Ind. Crops Prod.* **2010**, *32*, 627.
17. Nair, K. G.; Dufresne, A. *Biomacromolecules* **2003**, *4*, 666.
18. Bendahou, Y.; Habibi, H.; Kaddami, A.; Dufresne, A. *J. Biobased Mater. Bioenergy* **2009**, *3*, 81.
19. Angellier, H.; Molina-Boisseau, S.; Lebrun, L.; Dufresne, A. *Macromolecules* **2005**, *38*, 3783.
20. Angellier, H.; Molina-Boisseau, S.; Lebrun, L.; Dufresne, A. *Macromolecules* **2005**, *38*, 9161.
21. Valodkar, M.; Thakore, S. *J. Appl. Polym. Sci.* **2010**, *124*, 3815.
22. Valodkar, M.; Thakore, S. *Int. J. Polym. Anal. Char.* **2010**, *15*, 1.
23. Valodkar, M.; Thakore, S. *Carbohydr. Polym.* **2011**, *86*, 1244.
24. Yoshikai, K.; Oshakai, T.; Furukawa, M. *J. Appl. Polym. Sci.* **2002**, *85*, 2053.
25. Valodkar, M.; Thakore, S. *Carbohydr. Res.* **2010**, *345*, 2354.
26. Wu, Q.; Henriksson, M.; Liu, X.; Berglund, L. A. *Biomacromolecules* **2007**, *8*, 3687.
27. Sobkowicz, M. J.; Braun, B.; Dorgan, J. R. *Green Chem.* **2009**, *11*, 680.
28. Markovi, G.; Radovanovi, B.; Marinovi-Cincovi, M.; Budinski-Simendi, J. *Mater. Manuf. Process.* **2009**, *24*, 1224.
29. Namazi, H.; Dadkhah, A. *Carbohydr. Polym.* **2010**, *79*, 731.
30. Dufresne, A.; Cavaille, J. Y.; Helbert, W. *Macromolecules* **1996**, *29*, 7624.